

Study on the Conversion of Wool Keratin by Steam Explosion

Claudio Tonin,^{*,†} Marina Zoccola,[†] Annalisa Aluigi,[†] Alessio Varesano,[†]
Alessio Montarsolo,[†] Claudia Vineis,[†] and Francesco Zimbardi[‡]

CNR-ISMAR, Italian National Research Council, Institute for Macromolecular Studies, Biella, Italy and
ENEA, Italian Agency for New Technologies and the Environment, Biomass Unit, Rotondella, Italy

Received June 21, 2006; Revised Manuscript Received September 14, 2006

A wool fiber sample was submitted to chemical-free steam explosion in view of potential exploitation of keratin-based industrial and farm wastes. Fiber keratin was converted into a dark-yellow sludge that was submitted to phase separation by filtration, centrifugation, and precipitation of the soluble materials from the supernatant liquid. The resulting products, when compared with the original wool, showed the extent of disruption of the histology structure, reduction of the molecular weight to water-soluble peptides and free amino acids, and change of the structure of the remainder of the protein associated with breaking of disulfide bonds and decomposition of the high-sulfur-content protein fraction.

Introduction

Steam explosion is a rapidly developing technique for the efficient pretreatment of renewable resources into value-added materials for bioconversion. The process is based on short time steam cooking of biomasses at high temperature for several minutes, followed by explosive decompression. Steam explosion has been extensively studied since its invention in the early 1930s¹ because of the reduced refining energy consumption and high yield, combined with superior properties of the resulting products. This environmentally friendly technology currently finds industrial application² in pulping of lignocellulosic biomasses for paper, textile, and plastic industries^{3–4} as well as fractionation and extraction of fermentable sugars from corn stalks, wheat straw, and other agricultural wastes for the production of biofuel (ethanol) for energy use.^{5–6}

Keratin, one of the most abundant proteins, the major component of hair, feathers, wool, nails, and horns of mammals and birds, represents an important renewable biomaterial which can be better exploited.^{7–8} Moreover, disposal of keratin such as wool fiber waste from the textile industry, poor quality raw wools not fit for spinning, horns, nails, and feathers from butchery,⁹ estimated at more than 3 million tons per year,^{10–12} raises environmental and economic problems.^{13–14} These wastes could be recovered and transformed into new materials with innovative properties. For example, derivatives of protein hydrolysis (i.e., peptides or amino acids) currently find profitable applications in the cosmetic and detergency industry. Besides, research is in progress with the aim of producing innovative biomaterials suitable for novel “large-scale” uses in conventional fields (i.e., packaging, textiles, sanitary, filtration) or high-tech applications in niche sectors such as medical commodities and devices.^{15–16} In addition, it is known that keratinous materials can absorb toxic substances like heavy metal ions,^{17–24} formaldehyde, and other hazardous VOCs (volatile organic compounds);²⁵ thus, possible applications can be envisaged also in “active” water purification and air cleaning. Technical literature

reports on recent studies on the valorization of keratin wastes, mostly based on chemical cleavage of the disulfide bonds of the amino acid cystine, which are responsible for the high stability of keratins in order to extract soluble protein material which could be used for other applications.^{10–12,26–28} However, the reductive or oxidative agents used for S–S cleavage, namely, sulfites, thiols, or peroxides, are harmful, often toxic, and difficult to handle. Besides, the treatments result in severe degradation of the protein structure of keratin with reduction of the molecular weight and loss of mechanical properties.^{15–16,29–31}

This work deals with the characterization of the products resulting from the steam explosion of wool in a laboratory-scale plant. Treatment was performed chemical free, only with water vapor, in order to gather preliminary information in view of successive investigation on the environmentally friendly conversion process of keratin biomasses.

Experimental Section

Materials. Botany wool, 20.3 μm mean fiber diameter, in the form of tops (the sliver obtained from raw wool by scouring, carding, and combing processes) was supplied by The Woolmark Co., Italy. All chemicals were of analytical grade and purchased from Sigma-Aldrich, except otherwise specified.

Steam Explosion. Steam explosion of wool was carried out in a laboratory batch plant from STAKETECH (Canada). The reactor was a stainless-steel pressure vessel having a capacity of 10 L, surrounded by a steam jacket to prevent vapor condensation. The saturated steam used during the process was supplied by an external 16 kW boiler. A wet wool sample (100 g of wool impregnated with 300 g of water) was introduced into the reactor through a pneumatic loading valve and then soaked with saturated steam at 220 °C for 10 min. After the elapsed time, the blow valve was opened, the pressure decreased dramatically in a very short time, and the material discharged in a storage tank (150 L volume). A water condenser was connected with the storage tank in order to recover and remove as a liquid the volatile organic compounds produced during the process. A dark-yellow slurry (treated wool and condensed water) was recovered, closed in PE bottles, and frozen at –20 °C until the following analyses.

Separation and Identification of the Fractions. A 800 g amount of slurry (liquid and solid phases) from the steam explosion of wool

* To whom correspondence should be addressed. Phone: +39-0158493043. Fax: +39-0158408387. E-mail: c.tonin@bi.ismar.cnr.it.

[†] CNR-ISMAR.

[‡] ENEA.

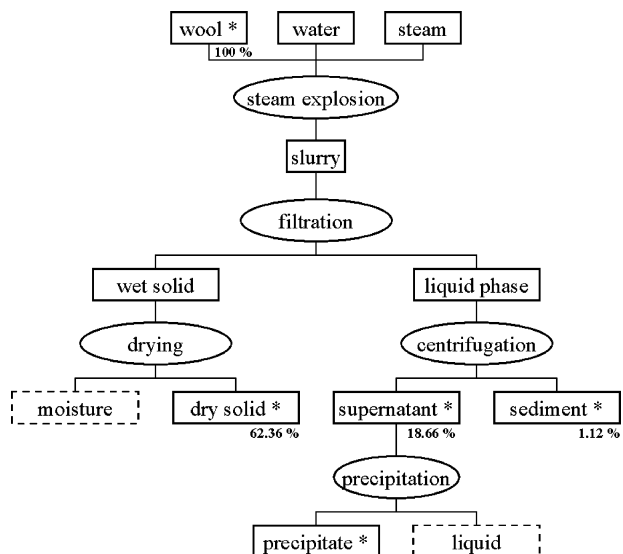


Figure 1. Diagram of the operations. The analyzed fractions are marked by asterisks. Percentages are the production yields of the fractions estimated with respect to the initial weight of wool.

was filtered by means of a 120 mesh stainless-steel filter, and the weight of the two phases was determined. Three samples of the wet solid were then dried in an oven at 105 °C until a constant weight was reached with the aim of evaluating the total moisture content. The rest of the wet solid was dried in a stove at 40 °C for 24 h and then conditioned at 20 °C, 65% R.H. Before further analysis, the dry solid was crushed in a mortar and solvent cleaned in a Soxhlet apparatus with dichloromethane and ethanol. The liquid phase was centrifuged at 14 000 rpm for 15 min. A low amount of sediment and a limpid, homogeneous, and yellow supernatant were obtained. The sediment was washed with ethanol and dried under low vacuum at room temperature. Proteins dissolved in the supernatant were precipitated and purified using acetone and then dried under low vacuum at room temperature (precipitate) for further analysis. Figure 1 shows a scheme of the operations described below that resulted in three different solid fractions, namely, the dry solid, sediment, and precipitate.

Morphological Characterization. Morphological studies were carried out by means of a Leica Electron Optics 135 VP scanning electron microscope (SEM). The investigation was performed with an acceleration voltage of 15 kV, 50 pA of current probe, and 30 mm of working distance. The samples were mounted on aluminum specimen stubs with double-sided adhesive tape and sputter-coated with a 20 nm thick gold layer in rarefied argon, using an Emitech K550 Sputter Coater, with a current of 20 mA for 180 s.

Amino Acid Analysis. Original wool, dry solid, sediment, precipitate, and supernatant were hydrolyzed with HCl (6 N) at 110 °C for 24 h in sealed tubes. Free amino acid residues were derivatized with hydroxysuccinimidyl carbamate (AQC by Waters) and eluted on a 15 × 0.39 cm reversed-phase column (Waters). An Alliance (Waters) high-performance liquid chromatograph (HPLC) was used, and the eluate was detected at 254 nm. The quantitative amino acid composition was determined by calibration with Amino Acid Standard H (Pierce) as external standard and α-aminobutyric acid as internal standard. The amount and composition of the free amino acid dissolved in the supernatant were determined directly before precipitation, thus avoiding the hydrolysis step.

SDS-PAGE Electrophoresis. Original wool, dry solid, sediment, and precipitate were subjected to extraction with dithiothreitol/urea solution containing Tris/HCl (550 mM pH 8.6), dithiothreitol (DTT; 140 mM), EDTA (5 mM), and urea (8 M) for 4 h under nitrogen atmosphere.³² The protein concentration of the wool extract was determined with the Bradford protein assay method (Bio-Rad) using bovine serum albumin as standard. SDS-PAGE was performed using a Xcell SureLock Mini-Cell (Invitrogen) on 12% polyacrilamide gels

capable of separating proteins with molecular weights between 188 000 and 3000 Da. Myosin, bovine serum albumin, glutamic dehydrogenase, alcohol dehydrogenase, carbonic anhydrase, myoglobin, lysozyme, aprotinin, and insulin were used as molecular weight markers.

FT-IR Spectroscopy. Fourier transform infrared (FT-IR) spectra of the solid fractions described above, dried at 105 °C for 2 h, were obtained from 4000 to 700 cm⁻¹ using the attenuated total reflectance (ATR) technique by a Nexus Thermo Nicolet Spectrometer. For each spectrum 100 scans were taken at a resolution of 4 cm⁻¹ and gain of 8.0. Spectra were baseline corrected, smoothed with a nine-point Savitsky–Golay function,³³ and normalized using the Amide I absorption intensity peak. The Amide I and Amide II bands were resolved by the second-order derivative with respect to the wavelength.

FT-NIR Spectroscopy. Fourier transform near infrared (FT-NIR) spectra of the solid fractions were collected in the region between 10 000 and 3700 cm⁻¹ using a Perkin-Elmer FT-NIR Spectrum IdentiCheck Spectrometer in the reflectance mode by means of the IdentiCheck reflectance accessory (ICRA). Each analytical spectrum was the result of the recording software combination of 32 scans.

Thermal Analysis. Differential scanning calorimetry (DSC) was performed with a Mettler Toledo DSC 821 calorimeter calibrated by an indium standard. The calorimeter cell was flushed with 100 mL min⁻¹ nitrogen. The runs were performed from 30 to 300 °C at a heating rate of 10 °C min⁻¹. The data were collected on a computer with the Mettler Toledo STARE System.

Results and Discussion

Steam Explosion Yield. The conversion yield of the original wool in the different fractions (as reported in Figure 1) was evaluated using the following equation

$$Y = \frac{W_{\text{sample}}}{W_{\text{drywool}}} 100 \quad (1)$$

where Y is the yield, W_{sample} is the weight of the related fraction, and W_{drywool} is the dry weight of the initial wool. The process produced 62.36% of dry solid, 18.66% of proteins dissolved in the supernatant (by amino acid analysis, HPLC), and 1.12% of sediment. Thus, in the experimental conditions, the process wastes about 17.9% of the initial dry wool weight also because of external factors such as incomplete recovery of the slurry and the presence of non-protein components in the wool (e.g., lipids and ash). All fractions, especially the supernatant, showed a dark-yellow color due to the presence of chromophores originating mainly from the aromatic amino acids (tryptophan, tyrosine, and phenylalanine) and smelt of sulfur because of the high content of the amino acid cystine in wool keratin.³⁴

Morphological Characterization. SEM investigation of the dry solid showed the presence of both wool fragments (Figure 2a) and shapeless aggregates (Figure 2) due to the strong thermal and pressure stresses the fibers were subjected to during the process. Fiber fragments were short (up to a few millimeters), but the typical scaled structure of the surface cuticle cells was still recognizable (Figure 2c). A micrograph of the sediment obtained by centrifugation of the liquid phase is reported in Figure 3. As can be seen, the sediment was mainly made of spherical particles with a diameter in the range from 0.5 to 3 μm, probably originated by the tendency of the protein to shrink when the fiber histology structure is disrupted by external thermal or chemical agents. A few small fiber fragments, not shown in this picture, were also detected. Moreover, SEM images revealed the absence of any residual histological structure of wool (e.g., cortical cells).

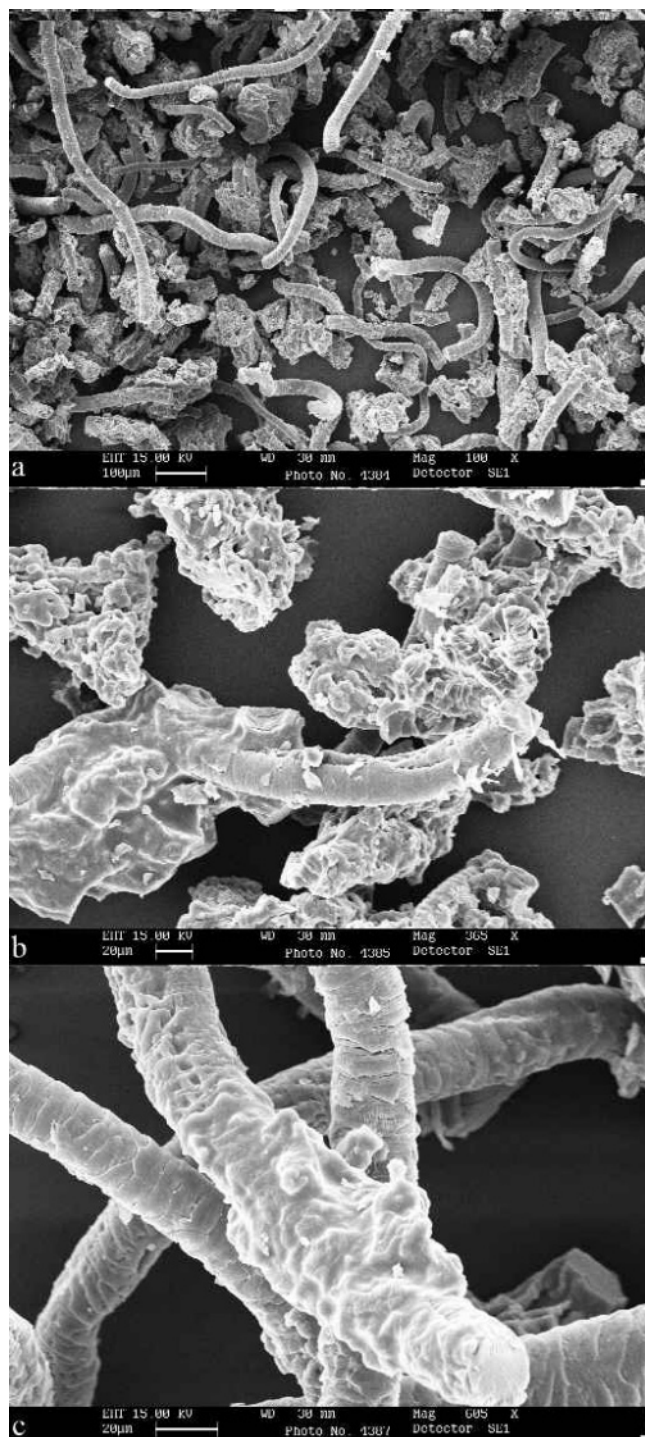


Figure 2. SEM pictures of the whole dry solid (a) constituted of keratin aggregates (b) and fiber segments (c).

Amino Acid Analysis. During HPLC preparative hydrolysis of keratins with HCl several amino acid residues undergo various degrees of degradation and conversion. Tryptophan residues are completely destroyed by the acidic conditions, methionine, cystine, cysteine, and tyrosine undergo partial degradation, while asparagine and glutamine residues are completely converted to aspartic and glutamic acid, respectively; cystine and cysteine are detected as 1/2 cystine.³⁰ Table 1 shows the results of the amino acid analysis of the steam-exploded wool fractions. Tyrosine values were a little lower in steam-exploded fractions than in the original wool, while phenylalanine values were unchanged. Tryptophan values were unavailable

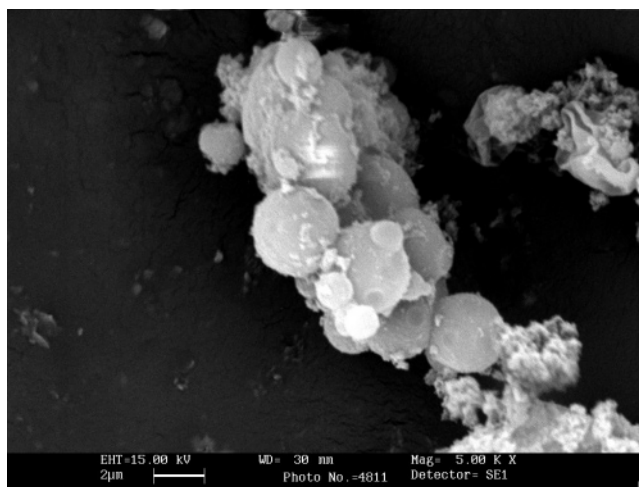


Figure 3. SEM picture of the spherical particles obtained in the sediment.

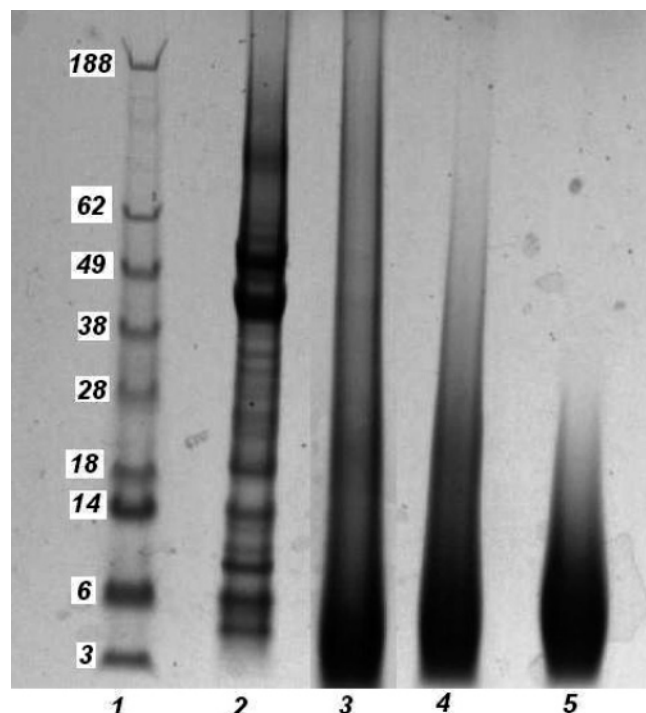
Table 1. Amino Acids composition (in mol % of the total protein concentration) of different fractions from the steam explosion of wool compared to reference wool

amino acids	wool	solid phase	sediment	precipitate	supernatant	free amino acids in supernatant
CYA	0.19	0.23	0.16	0.11	0.25	0.90
ASP	7.69	8.73	9.00	9.15	6.80	26.89
SER	10.57	10.41	9.58	8.15	10.02	15.86
GLU	13.05	14.68	16.23	18.52	14.73	2.39
GLY	8.21	9.88	9.25	7.31	10.00	10.47
HIS	0.80	0.85	0.83	0.80	1.07	1.68
ARG	6.43	6.45	7.31	6.74	7.33	3.90
THR	6.59	6.22	6.00	5.85	6.56	1.84
ALA	5.36	6.25	6.44	7.61	7.41	12.82
PRO	6.36	6.46	5.45	5.49	7.17	8.07
1/2CYS	10.20	3.09	1.54	1.23	1.12	0.00
TYR	3.19	3.03	3.20	2.29	2.50	1.84
VAL	5.55	6.04	6.24	6.89	6.86	3.69
MET	0.38	0.31	0.52	0.60	0.64	0.00
LYS	3.15	4.02	3.78	4.03	2.79	1.01
ILE	3.09	3.34	3.74	4.11	3.78	2.46
LEU	7.05	7.62	8.35	9.46	8.85	4.80
PHE	2.16	2.41	2.39	1.70	2.13	1.38

because tryptophan was completely destroyed. Wool keratin contains a large number of disulfide bonds, associated with the amino acid cystine, which cross-link the protein chains. Disulfide bonds are responsible for the higher stability and lower solubility of keratin compared with most proteins. The amount of 1/2 cystine found in the different solid fractions was very low compared to the original wool. Most of the cystine was destroyed because of the temperature of the process.³⁰ Indeed, only a very small amount of cysteic acid, characteristic of undamaged wool, was found. Moreover, breaking of disulfide bonds as a result of cystine destruction combined with breaking of peptide bonds shown by electrophoresis (see below) caused a considerable amount of peptides and free amino acids to be dissolved in water. The concentrations of 25 and 0.16 g L⁻¹ were determined, respectively, for peptides and free amino acids dissolved in the supernatant, corresponding to 18.66 wt % of the original wool. This is in good accordance with the yield calculated by weighting the solid fractions if one considers that many external factors can have an influence on the process yield: (1) incomplete recovery of the slurry stuck to the walls of the storage tank; (2) the presence of non-protein components in the original wool sliver (principally small amounts of lipids and ash); (3) some amino acids were destroyed or degraded by the steam explosion process itself or by the HPLC preparative acid hydrolysis. Table 2 shows the ratio of hydrophilic (aspartic

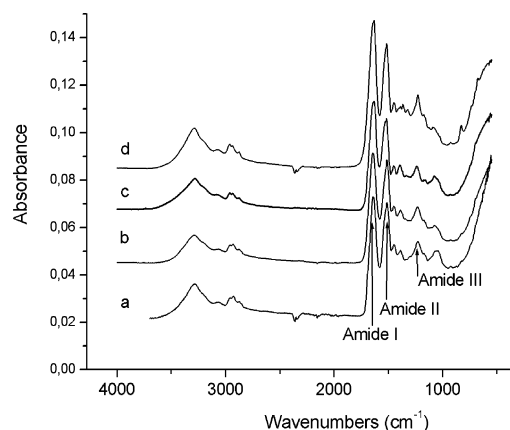
Table 2. Percentage of Amino Acids with Hydrophilic and Hydrophobic Side Groups for Reference Wool and Different Fractions from Steam Explosion of Wool

sample	hydrophilic ^a (% mol)	hydrophobic ^b (% mol)	hydrophilic/ hydrophobic ratio
wool	31.12	18.23	1.7
solid phase	34.73	19.72	1.8
sediment	37.15	21.24	1.7
precipitate	39.24	22.76	1.7
supernatant	32.72	22.26	1.5
free amino acids in supernatant	35.87	12.33	2.9

^a Asp, Glu, His, Arg, Lys. ^b Val, Leu, Ile, Met, Phe.**Figure 4.** Electrophoretic separation patterns (SDS-PAGE) samples: lane 1, MW standard; lane 2, DTT/urea wool extract; lane 3, solid phase; lane 4, sediment; lane 5, precipitate.

acid, glutamic acid, histidine, arginine, and lysine) to hydrophobic (valine, leucine, isoleucine, methionine, and phenylalanine) amino acids calculated for steam-exploded fractions. As a result, the original wool and different solid fractions contained a majority of amino acids with hydrophilic side groups, while free amino acids dissolved in the supernatant were still more hydrophilic.

SDS-PAGE Electrophoresis. Figure 4 reports the electrophoresis separation patterns of the keratins extracted with DTT/urea from dry solid, sediment, and precipitate compared with those extracted from the original wool as a reference. The original wool (lane 2) typically shows two important keratin fractions that are the low-sulfur (LS) proteins of the intermediate filaments, whose molecular weight falls in the range of 67–43 kDa, and the high-sulfur (HS) proteins of the matrix, whose molecular weight falls in the range 28–11 kDa. The electrophoresis patterns of the dry solid, sediment, and precipitate (reported in lanes 3, 4, and 5, respectively) show that the strong bands of LS proteins disappeared. Therefore, bands of high protein density appeared in the low fractionation range at around 18–3 kDa for the dry solid and sediment and around 14–3

**Figure 5.** Spectra (4000–800 cm^{-1}) of wool (a) and samples of steam explosion process: solid phase (b), sediment (c), precipitate (d).

kDa for the precipitate. The loss of high molecular weight keratin indicates that the chemical structure was significantly affected by the high temperature of the steam explosion.

FT-IR Spectroscopy. Figure 5 reports the FT-IR spectra of the original wool (trace a) and the products resulting from the steam explosion treatment (traces b, c, and d for dry solid, sediment, and precipitate, respectively). All spectra show absorption bands in the 4000–2800 cm^{-1} region. The Amide A (3282 cm^{-1}) and Amide B (3065 cm^{-1}) bands are connected with the frequency of N–H stretching vibrations; Fermi resonance between the first overtone of Amide II influences these bands.³⁵ Bands that fall in the 3000–2800 cm^{-1} range are related to C–H stretching modes. However, keratin absorptions at 1650, 1540, and 1250 cm^{-1} that dominate the mid-infrared spectrum and designated, respectively, as Amide I, II, and III are often used to study conformational arrangements of proteins. Amide III is a more complex vibrational mode deriving from in-phase combination of N–H in-plane bending and C–N stretching with contributions from C–C stretching and C–O bending. Therefore, it is very hard to find out correlations between the Amide III band shape and protein secondary structure.³⁶ Otherwise, Amide I and Amide II bands can be used to extract information about the secondary structure of the protein.^{37,38} Amide I absorption arises primarily from the C=O stretching vibration, while Amide II derives mainly from in-plane N–H bending (40–60% of the potential energy) with minor contributions of C–N (18–40%) and C–C (about 10%) stretching vibrations.

The broad Amide I and II bands of all samples were resolved by the second-order derivative;³⁹ it should be noted that the peak positions are inverted in the second-order spectra (Figure 6). With respect to the original wool (trace a), the absorptions for Amide I at 1650 cm^{-1} and for Amide II at 1549 cm^{-1} suggest a significant proportion of α -helix structure, which characterizes the intermediate filaments proteins, whereas the second weaker Amide I maximum at 1627 cm^{-1} and the peaks at low intensity in the 1695–1680 cm^{-1} range indicate, respectively, some degree of β -sheet and disordered keratin conformations that are typical of the cuticle cells (which constitute the outer layer of wool fiber) and the matrix that surrounds the intermediate filaments.⁴⁰ In the resolved Amide I of the steam-exploded samples (traces b, c, d) it is worth noting a significant decrease in the intensity of the absorption band at 1650 cm^{-1} with respect to the 1627 cm^{-1} band coupled with a significant decrease of the Amide II components at 1549 cm^{-1} with respect to the component at 1512 cm^{-1} .

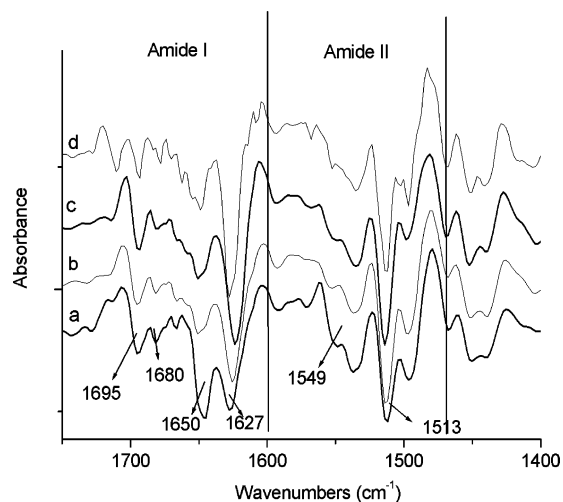


Figure 6. Second-derivative infrared spectra (1750–1400 cm^{-1}) of reference wool (a) and steam explosion samples: solid phase (b), sediment (c), precipitate (d).

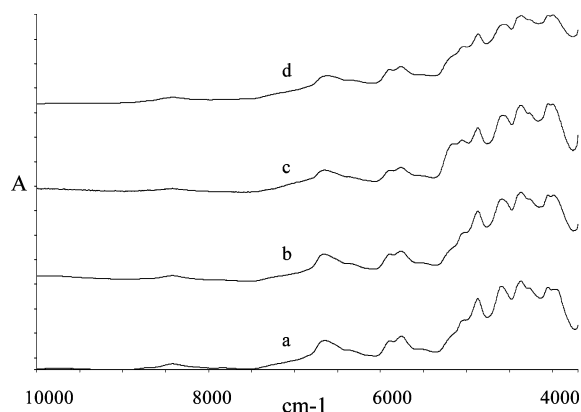


Figure 7. Near-infrared spectra of reference wool (a), solid phase (b), sediment (c), and precipitate (d).

This means that a lower α -helical structure amount was contained in the products resulting from steam explosion with respect to the original wool and degraded proteins tend to assume a β -sheet and disordered structures. Moreover, changes in the molecular weight distributions and the amino acid composition (i.e., the decrease of the cystine content) suggest changes in the protein chains rearrangements.

FT-NIR Spectroscopy. The absorption bands in the NIR region (between 13 000 and 4000 cm^{-1}) are the result of overtones and combinations originating in the fundamental midrange infrared region of the spectrum. The bonds involved are generally C–H, N–H, O–H, and S–H.⁴¹ Figure 7 shows the NIR spectra of the original wool and products of the steam explosion. The doublet at about 5800 cm^{-1} is the overtone of the C–H stretch of protein side chains and lipids, and the bands between 5000 and 3700 cm^{-1} give information about the protein-type structure of the material. Anyway, just small differences were found between the spectra that were mainly attributed to preparation and drying techniques.

Therefore, in order to obtain more structural information the second-derivate spectra were obtained in the region between 5000 and 4000 cm^{-1} (Figure 8). One strong band (4860 cm^{-1}), assignable to the Amide A–Amide II combination, was observed in each derivative spectra. Besides, the band at 4600 cm^{-1} in the original spectra, assignable to the Amide B–Amide II combination, was boarder in the dry solid, sediment, and precipitate than in the original wool. The second-derivative

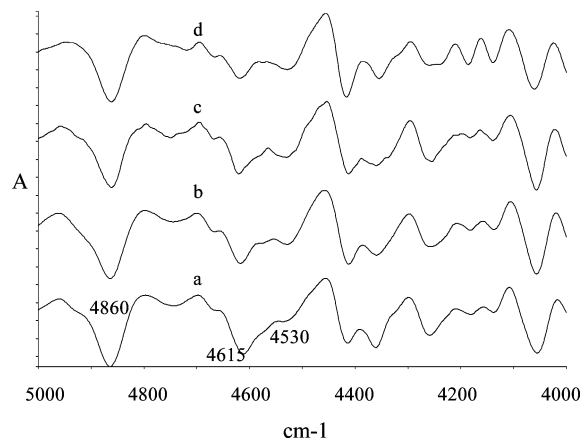


Figure 8. Second derivative of NIR spectra of reference wool (a), solid phase (b), sediment (c), and precipitate (d).

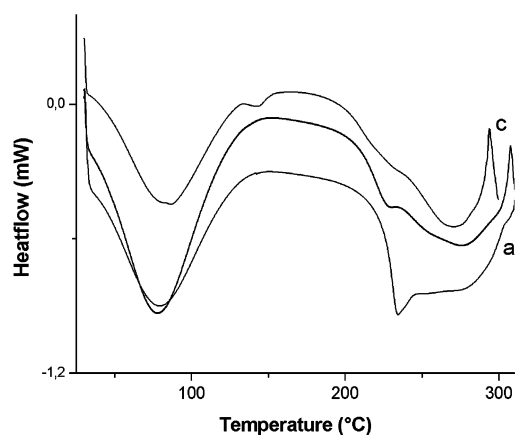


Figure 9. DSC curves of untreated wool (a), solid phase (b), and sediment (c).

procedures divided this absorption band into two bands at 4615 and 4530 cm^{-1} , respectively, and the second one, at 4530 cm^{-1} , was higher than those of the reference original wool. This band, which was found in many di- to hexapeptides and in proteins rich in β -sheet structures (e.g., native silk fibroin), would appear to be assignable to any non- α -helical structure.⁴² In accordance with the results obtained in the midinfrared region, steam explosion causes changes in the secondary structure of wool proteins and in their ordered α -helical structure as well, leading to a β -sheet or more disordered structures. The region between 4500 and 4000 cm^{-1} is influenced by the various C–H combination bands of side chains of amino acids in proteins. Changes in absorption intensities or bands shifting were found between different spectra from solid phase, sediment, precipitate, and reference wool.

Thermal Analysis. In Figure 9 the DSC thermograms of the dry solid (b) and sediment (c) are compared with those of the original wool (a). The large endotherm peak which falls at around 60 $^{\circ}\text{C}$ originates from water evaporation; instead, characteristic thermal events take place in the 200–300 $^{\circ}\text{C}$ range. As is well documented in literature, the original wool shows a bimodal endothermic peak in the temperature range 230–240 $^{\circ}\text{C}$ due to thermal denaturation of the α -helical crystallites (234 $^{\circ}\text{C}$), overlapped by the degradation of other histological components, namely, the cystine-rich matrix (the presence of a shoulder in the higher temperature side of the trace),^{43–47} and denaturation of other histological components are observed around 270 $^{\circ}\text{C}$. The dry solid and sediment show the helical denaturation peak shifted at lower temperature

associated with a decrease of the underlying area. The shift at lower temperature could be caused by reduction of the cystine content that occurs in the treated samples;^{43,44} furthermore, the area decrease is further support of the lesser α -helix content in the products of steam explosion with respect to the untreated original wool due to the transition of the α -form crystallites in β -pleated sheet structures,⁴⁵ similar to those found in silk fibroin and feather keratins.

Conclusions

Preliminary investigation on the steam explosion of wool with water vapor showed the nature and extent of the conversion of fiber keratin by effect of the strong physical condition of the process. The resulting products, besides the modification of the histology and structural assembly of the original material, show a strong decrease of disulfide bonds associated with the amino acid cystine, which cross-link the protein chains and thus are responsible for the higher stability and lower solubility of keratin compared with most proteins. Cleavage of the disulfide bonds without the use of harmful, often toxic reductive or oxidative agents allows the extraction of protein material from keratin wastes, susceptible of larger exploitation and valorization.

Acknowledgment. The authors greatly acknowledge CAR-IPLO Foundation (Milan, Italy) for financial support within the research project "New fibres from renewable resources: fibres on demand".

References and Notes

- (1) Mason, W. H. U.S. Patent 1655618, 1928.
- (2) Focher, B.; Marzetti, A.; Crescenzi, V. *Steam Explosion Techniques: Fundamentals and Industrial Applications*; Gordon & Breach Scientific Publishers Ltd.: Philadelphia, 1991.
- (3) Ahring, B. K.; Thomsen, A. B. U.S. Patent 20020192774, 2002.
- (4) Young, R. A.; Aktar, M. *Environmentally friendly technologies for pulp and paper industries*; John Wiley & Sons, Inc.: New York, 1998.
- (5) Johnson, D. K.; Chornet, E.; Zmierzak, W.; Shabtai, J. *Prepr. Pap.—Am. Chem. Soc., Div. Fuel Chem.* **2002**, 47, 380–381.
- (6) McKendry, P. *Biores. Technol.* **2002**, 83, 47–54.
- (7) Onifade, A. A.; Al-Sane, N. A.; Al-Musallam, A. A.; Al-Zarban, S. *Biores. Technol.* **1998**, 66, 1–11.
- (8) Schrooyen, P. M. M.; Dijkstra, P. J.; Oberthür, R. C.; Bantjes, A.; Feijen, J. *J. Colloid Interface Sci.* **2001**, 240, 30–39.
- (9) Salminen, E.; Rintala, J. *Biores. Technol.* **2002**, 83, 13–26.
- (10) Garzena, F. Fiber artificiali: da chardonnnet alla cheratina. Degree thesis, Politecnico di Torino, Italy, 2003.
- (11) Jacques, C. Etude de la valorisation des déchets d'origine keratinique par voie thermo-mecano-chimique en vue de l'obtention de filaments continus: cas spécifique de la laine. Ph.D. thesis, Institut national polytechnique de Toulouse, France, 2003.
- (12) Schmidt, W.F. Innovative feather utilization strategies, *Proceedings of the National Poultry Waste Management Symposium*, Oct 19–22, 1998, Springdale, AR; pp 276–282.
- (13) Moncrieff, R. W. *Man-Made Fibers*, 6th ed; Butterworths Scientific: London, 1975.
- (14) Woodings, C. *Regenerated Cellulose Fibres*; Woodhead Publishing: Cambridge, 2001.
- (15) Aluigi, A.; Innocenti, R.; Tonin, C.; Vineis, C.; Freddi, G. *AUTEX Res. J.* **2004**, 4, 175–181.
- (16) Vineis, C.; Aluigi, A.; Montarsolo, A.; Varesano, A.; Mazzuchetti, G.; Tonin, C.; Ferrero, F. Nanofibres of wool keratin/poly(ethylene oxide) blends for biomedical applications. *Proceedings of the 6th Textile and Health International Forum*, May 4–5, 2006, Biella, Italy.
- (17) Misra, M.; Kar, P.; Homonoff, E.C.; Licata, C. AKF Keratin-Protein Fiber as a Bisorbent for Heavy Metals from Solutions. *American Filtration and Separation Society Annual Meeting*, April 30–May 4, 2001, Tampa, FL.
- (18) Kar, P.; Misra, M. *J. Chem. Technol. Biotechnol.* **2004**, 79, 1313–1319.
- (19) Kokot, S. *Textile Res. J.* **1993**, 63, 159–161.
- (20) Masri, S. M.; Friedman, M. *Adv. Exp. Med. Biol.* **1974**, 48, 551–587.
- (21) Hartley, F. R. *Aust. J. Chem.* **1968**, 21, 1013–1022.
- (22) Guthrie, R. E.; Laurie, S. H. *Aust. J. Chem.* **1968**, 21, 2437–2443.
- (23) Hamrajani, S. N.; Narwani, C. S. *J. Indian Chem. Soc.* **1967**, 44, 704–709.
- (24) Hojo, N. *Sen-I Gakkaishi* **1958**, 14, 953–955.
- (25) Tonin, C. Italian Patent TO2003A000259, 2003.
- (26) Tanabe, T.; Okitsu, N.; Tachibana, A.; Yamauchi, K. *Biomaterials* **2002**, 23, 817–825.
- (27) Tanabe, T.; Okitsu, N.; Yamauchi, K. *Mater. Sci. Eng. C* **2004**, 24, 441–446.
- (28) Katoh, K.; Shibayama, M.; Tanabe, T.; Yamauchi, K. *Biomaterials* **2004**, 25, 2265–2272.
- (29) Ley, K. F.; Marshall, R. C.; Crewther, W. G. Further studies on the release and characterisation of cuticle and membranous components from wool. *Proceedings of the 7th International Wool Textile Conference*, 1985, Tokyo, I; pp 152–161.
- (30) Maclaren, J. A.; Milligan, B. *Wool Science*; Science Press: Marriickville, Australia, 1981.
- (31) Tonin, C.; Aluigi, A.; Vineis, C.; Varesano, A.; Montarsolo, A.; Ferrero, F. *J. Therm. Anal. Cal.* **2006**, in press.
- (32) Marshall, R. C. *Textile Res. J.* **1981**, 51, 106–108.
- (33) Savitzky, A.; Golay, J. E. *Anal. Chem.* **1964**, 36, 1628–1639.
- (34) Smith, G. J. *J. Photochem. Photobiol. B: Biol.* **1995**, 27, 187–198.
- (35) Wojciechowska, E.; Włochowicz, A.; Weselucha-Birczyńska, A. *J. Mol. Struct.* **1999**, 511–512, 307–318.
- (36) Griebenow, K.; Santos, A. M.; Carrasquillo, K. G. *Internet J. Vib. Spec.* **1998**, 1, 3, 1.
- (37) Surewicz, W. K.; Mantsch, H. H.; Chapman, D. *Biochemistry* **1993**, 32, 389–394.
- (38) Jackson, M.; Mantsch, H. H. *Crit. Rev. Biochem. Mol. Biol.* **1995**, 30, 95–120.
- (39) Dong, A.; Huang, P.; Caughey, W. S. *Biochemistry* **1990**, 29, 3303–3308.
- (40) Wojciechowska, E.; Rom, M.; Włochowicz, A.; Wysocki, M.; Weselucha-Birczyńska, A. *J. Mol. Struct.* **2004**, 704, 315–321.
- (41) Burns, D. A.; Ciurczak, E. V. *Handbook of Near-Infrared Analysis*; Marcel Dekker: New York, 1992.
- (42) Miyazawa, M.; Sonoyama, M. *J. Near Infrared Spectrosc.* **1998**, 6, A253–A257.
- (43) Spei, M.; Holzem, R. *Colloid Polym. Sci.* **1987**, 265, 965–970.
- (44) Spei, M.; Holzem, R. *Melliand Textilberichte* **1991**, 6, 431–439.
- (45) Cao, J. *J. Appl. Polym. Sci.* **1997**, 63, 411–415.
- (46) Wortmann, F.-J.; Deutz, H. *J. Appl. Polym. Sci.* **1998**, 68, 1991–1995.
- (47) Tonin, C.; Aluigi, A.; Bianchetto, M.; D'Arrigo, C.; Mormino, M.; Vineis, C. *J. Therm. Anal. Cal.* **2004**, 77, 987–996.

BM060597W